Dentomaxillofacial Radiology (2019) 48, 20170344

birpublications.org/dmfr

RESEARCH ARTICLE

Osteoporosis detection in panoramic radiographs using a deep convolutional neural network-based computer-assisted diagnosis system: a preliminary study

[1]Jae-Seo Lee, [2]Shyam Adhikari, [1]Liu Liu, [3]Ho-Gul Jeong, [2]Hyongsuk Kim and [1]Suk-Ja Yoon

[1]Department of Oral and Maxillofacial Radiology, School of Dentistry, Dental Science Research Institute, Chonnam National University, Gwangju, South Korea; [2]Division of Electronics Engineering, Chonbuk National University, Jeonju, South Korea; [3]Dental Imaging Research Center, Medipartner, Seoul, South Korea

Objectives To evaluate the diagnostic performance of a deep convolutional neural network (DCNN)-based computer-assisted diagnosis (CAD) system in the detection of osteoporosis on panoramic radiographs, through a comparison with diagnoses made by oral and maxillofacial radiologists.

Methods: Oral and maxillofacial radiologists with >10 years of experience reviewed the panoramic radiographs of 1268 females {mean [± standard deviation (SD)] age: 52.5 ± 22.3 years} and made a diagnosis of osteoporosis when cortical erosion of the mandibular inferior cortex was observed. Among the females, 635 had no osteoporosis [mean (± SD) age: 32.8 ± SD 12.1 years] and 633 had osteoporosis (72.2 ± 8.5 years). All panoramic radiographs were analysed using three CAD systems, single-column DCNN (SC-DCNN), single-column with data augmentation DCNN (SC-DCNN Augment) and multicolumn DCNN (MC-DCNN). Among the radiographs, 200 panoramic radiographs [mean (± SD) patient age: 63.9 ± 10.7 years] were used for testing the performance of the DCNN in detecting osteoporosis in this study. The diagnostic performance of the DCNN-based CAD system was assessed by receiver operating characteristic (ROC) analysis.

Results: The area under the curve (AUC) values obtained using SC-DCNN, SC-DCNN (Augment) and MC-DCNN were 0.9763, 0.9991 and 0.9987, respectively.

Conclusions: The DCNN-based CAD system showed high agreement with experienced oral and maxillofacial radiologists in detecting osteoporosis. A DCNN-based CAD system could provide information to dentists for the early detection of osteoporosis, and asymptomatic patients with osteoporosis can then be referred to the appropriate medical professionals.
Dentomaxillofacial Radiology (2019) **48**, 20170344. doi: 10.1259/dmfr.20170344

Cite this article as: Lee J-S, Adhikari S, Liu L, Jeong H-G, Kim H, Yoon S-J. Osteoporosis detection in panoramic radiographs using a deep convolutional neural network-based computer-assisted diagnosis system: a preliminary study. *Dentomaxillofac Radiol* 2019; **48**: 20170344.

Keywords: panoramic radiograph; computer-assisted diagnosis; osteoporosis

Introduction

Osteoporosis is defined by low bone mass and microarchitectural deterioration of bone tissue, which leads to bone fragility and increased fracture risk.[1] Disability following hip, vertebral and wrist fractures can reduce the quality of life of patients and lead to increased financial burden on health-care systems.[2] Moreover, mortality risk following osteoporosis-related fracture increases.[2–5]

The prevalence of osteoporosis in the EU ranged from 5.7% in Slovakia to 6.9% in Greece, Italy and Sweden for males aged ≥50 years and from 19.3% in

Correspondence to: Professor Hyongsuk Kim, E-mail: hskim@jbnu.ac.kr; Professor Suk-Ja Yoon, E-mail: yoonfr@jnu.ac.kr

Received 08 September 2017; revised 25 June 2018; accepted 26 June 2018
The authors Jae-Seo Lee and Shyam Adhikari contributed equally to the work.

Cyprus to 23.4% in Italy for females.[3] The prevalence of osteoporosis in the United States was estimated at 2% for males and 11% for females.[6] The prevalence of osteoporosis in the Republic of Korea is higher than that in other countries; 7.5% of Korean males and 37.5% of Korean females aged >50 years have osteoporosis.[7]

The US Preventive Services Task Force found credible evidence that indicates a reduction in subsequent fracture rates among post-menopausal females who received treatment. The benefit of treating screening-detected osteoporosis is shown to be at least moderate for females aged ≥65 years and younger females, with similar fracture risk estimates.[8]

Dual energy X-ray absorptiometry (DXA) is an effective measure to identify bone mineral density (BMD) and is used to diagnose osteoporosis and for osteoporosis-related fracture risk prediction.[9,10] However, the cost of a DXA scan is relatively high and the use of DXA machines is limited in most developing Asian countries.[11] In contrast, an increasing life expectancy has led to the wide use of panoramic radiography in dental treatment for elderly patients; panoramic radiography is cost-efficient for detecting osteoporotic changes.[12]

Previous studies proved the significant association between mandibular cortical shape on panoramic radiographs and skeletal BMD on DXA in post-menopausal females.[13–18] Panoramic radiographic indexes such as the Gonion index, mandibular cortical index (MCI), mental index and panoramic mandibular index were used for detecting osteoporosis.[13–17,19–23] Previous studies suggested that dentists should be able to refer patients to medical professionals for appropriate treatments when osteoporosis is suspected, based on panoramic radiography assessment.[13,15,21,24]

However, it is not easy for dentists to screen for osteoporosis based on panoramic radiography, as general dentists typically focus on dental problems. A previous study reported that oral and maxillofacial radiologists may have better performance of diagnosing osteoporosis than general dentists.[25] Therefore, several methods of computer-assisted diagnosis (CAD) for osteoporosis that use, for example, a classifier system such as a random forest classifier support vector machine based on bone features, have been developed.[26,27] A fuzzy neural network[28] and hybrid genetic swarm fuzzy classifier model[29] were also developed. These methods utilize machine learning, which is a subgroup of artificial intelligence (AI). Generally, AI has several major types, including symbolic AI (rule-based; *e.g.* IBM Watson), connectionist AI (network- and connection-based; *e.g.* deep learning or artificial neural net) and evolutionary AI (genetic algorithms).[30]

In the ImageNet Large Scale Visual Recognition Challenge, deep learning methods revealed the best performance for the classification of images.[31] Since 2012, the deep convolutional neural network (DCNN), which is a deep-learning approach to optimizing image recognition, was used in all winning entries.[32] Deep learning-based computer-aided diagnosis for breast cancer,[33] lung cancer[34] and Alzheimer's disease[35] has been applied in radiology. However, to the best of our knowledge, only a few studies on the DCNN-based CAD system have been conducted in dental radiology. The purpose of this study was to evaluate the diagnostic performance of the DCNN-based CAD system in the detection of osteoporosis in panoramic radiographs, through a comparison with diagnoses (the gold standard) made by oral and maxillofacial radiologists.

Methods and materials

The study protocol was approved by the institutional review board (CNUDH-2017–014) of Chonnam National University Dental Hospital.

Study population

The study subjects were females {mean [± standard deviation (SD)] age: 52.5 ± 22.3 years} who visited Chonnam National University Dental Hospital between 2009 and 2016. They underwent a digital panoramic radiography evaluation as part of their dental examination. All panoramic radiographs were acquired using Kodak 8000C digital panoramic equipment (Carestream Health Inc., Rochester, NY) set at 71 kVp and 12 mA for 13.2 s.

Evaluation of panoramic radiographs

All panoramic radiographs were examined by two oral and maxillofacial radiologists with over 10 years of experience. All images were evaluated using PiViewStar PACS (Infinitt, Seoul, Korea) and an LCD monitor with a screen resolution of 2048 × 2560 (IF2105MP; WIDE, Seoul, Korea). Both observers (Yoon and Lee) interpreted the MCI of each panoramic radiograph independently, in accordance with the classification of Klemetti et al.[19] The MCI was classified as one of three groups, namely C1, C2 and C3. C1 is a normal mandibular cortex, with an even and sharp mandibular endosteal margin; C2 is a mildly or moderately eroded cortex, with a mandibular endosteal margin presenting semilunar defects or appearing to form cortical residues; C3 is a severely eroded cortex, with a mandibular cortical layer forming heavy endosteal cortical residues, and the bone is clearly porous.

In this study, the final diagnosis was made when two observers agreed, and a diagnosis of osteoporosis was made when cortical erosion was observed (either of the C2 or C3 type according to the classification of Klemetti et al).[19]

The static for intra-observer and inter-observer agreements were as follows: Yoon-Yoon, intrapersonal agreements Kappa value = 1; Lee-Lee, intrapersonal agreements Kappa value = 0.98; Yoon-Lee, first round interpersonal agreement Kappa value = 0.96; Yoon-Lee,

second round interpersonal agreement Kappa value = 0.98.

We randomly selected 1,500 panoramic radiographs taken between 2008 and 2016 from Chonnam National University Dental Hospital's Picture Archiving and Communication System (PACS), based on their oral and maxillofacial radiologist report. A total of 232 panoramic radiographs were excluded.

The selection criteria of the panoramic radiographs were as follows: no pathological bone change or surgery history on the mandible; the patient had no systematic disease except osteoporosis; and the panoramic radiograph was of good quality (clear appearance of the mandibular border and proper positioning of patient).

Based on the selection criteria, panoramic radiographs from 1268 dental patients [mean (± SD) age: 52.5 ± 22.3 years] were included in the study. Among the patients, 635 had no osteoporosis [mean (± SD) age: 32.8 ± 12.1 years] and 633 had osteoporosis (72.2 ± 8.5 years). In neural network training, the amount of data for each class should be nearly balanced; otherwise, the neural training is influenced too heavily by the class with the majority of data while the other class is not weighted sufficiently.

The dataset was divided into training, validation and test sets as follows: The radiographs were selected randomly, and 200 radiographs [patient age >50 years; number of normal radiographs: 100; mean (± SD) patient age: 55.4 ± 5.8 years; number of radiographs from patients with osteoporosis: 100; mean (± SD) age: 72.4 ± 7.1 years] were set aside as a test set. The remaining 1068 radiographs [normal, 535; mean (± SD) patient age: 28.6 ± 7.4 years and with osteoporosis, 533; mean (± SD) patient age: 72.1 ± 8.7 years] were used for training and data validation.

Pre-processing of the panoramic radiographs

The panoramic radiographs had a uniform height of 1244 pixels but varied in width, ranging from 2411 to 2628 pixels. For efficient processing in terms of computation and memory requirements, the images were down-sampled to a uniform size of 1240 × 680 pixels (Figure 1) using bilinear interpolation.

Deep convolutional neural network architecture

Two methods, single-column deep convolutional neural network (SC-DCNN) and multicolumn deep convolutional neural network (MC-DCNN), were used for training, validating and testing the convolutional neural network in detecting osteoporosis on panoramic radiographs.

Single-column deep convolutional neural network: In the first method, the SC-DCNN was restricted to the region of interest (ROI), which was the mandible below the teeth-containing alveolar bone, for an image size of 1000 × 200 pixels. A simple pre-processing approach of zero-centring the data was used, and the mean of the training data was calculated and subtracted from all the image pixels (Figure 1).

The architecture of SC-DCNN was established according to the flagship AlexNet model.[36] The input to the network was the grey level of the ROI within the 1000 × 200 pixel area, and the output of the network was the conditional probability distribution $p(Y|X)$ over the two categories, "osteoporosis" and "normal." The network consists of a stack of five convolutional layers, where each convolutional layer (Conv) is followed by a max pooling layer (Pool) and then by a ReLU[37] activation layer. The size of the kernels used in the convolutional layers were 5 × 5, 5 × 5, 3 × 3 and 3 × 3, in that order. The fifth convolutional layer was followed by three fully connected layers with a Softmax classifier on

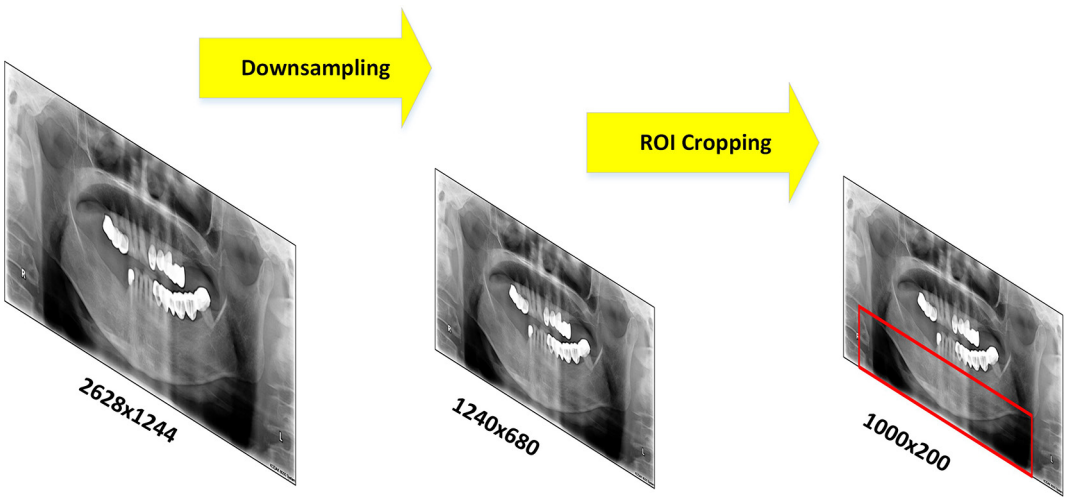

Figure 1 Data preparation for the SC-DCNN. The original radiography image is down-sampled, and the ROI is restricted to the mandibular region below the teeth (region inside the bounding box). ROI, region of interest; SC-DCNN, single-column deep convolutional neural network.

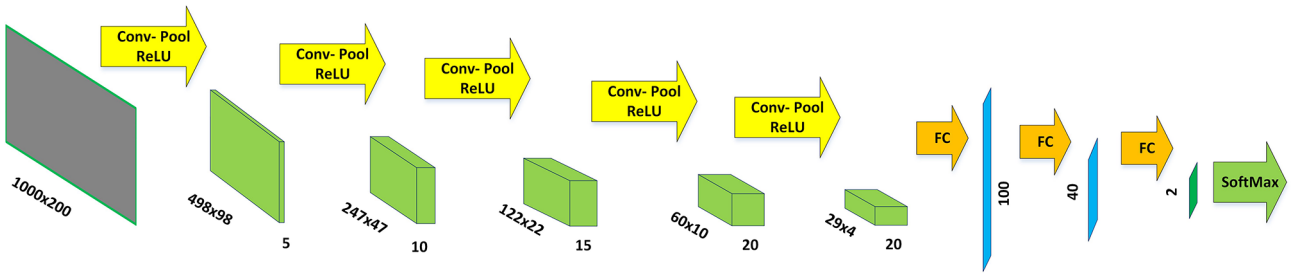

Figure 2 Single-column deep convolutional neural network (SC-DCNN).

top. The topmost layer (or output layer) was a Softmax classifier, which is a generalisation of the logistic function and normalised exponential function that converts a K-dimensional vector of arbitrary real values to a K-dimensional vector of real values in the range (0,1) that add up to 1. The function is given by the following equation (1) :

$$\left(Y = i|x, W, b\right) = softmax_i \left(Wx + b\right) = \frac{e^{W_i x + b_i}}{\sum_j e^{W_j x + b_j}}$$

The output of the Softmax layer was the conditional probability distribution over the two target classes, and the interpretation of the model was the class with the maximum probability (Figure 2).

Multicolumn deep convolutional neural network: Two ROIs, the right and left mandibular body areas, were extracted on each panoramic radiograph, resulting in two 400 × 200 pixel ROIs. A simple pre-processing approach of zero-centring the data, as explained earlier, was used (Figure 3).

An MC-DCNN was established using the two ROIs as input. Each column processed a different ROI. The input to the left column was the left ROI, and the input to the right column was the right ROI. Similar to that in the SC-DCNN, each column in this network consisted of a stack of five convolutional layers, where each convolutional layer (Conv) was followed by a max pooling layer (Pool) and a ReLU activation layer. The feature maps of the fifth convolutional layers from the left and right columns of the network were concatenated and fed-forward through three fully connected layers with a Softmax classifier at the output. The output of the Softmax was again the conditional probability distribution over the two target classes, and the final interpretation of the model was the class with the maximum probability. The multicolumn structure allowed for the learning of the left and right ROI-specific features separately, and the classifier on the top used features from both ROIs to make the final interpretation (Figure 4).

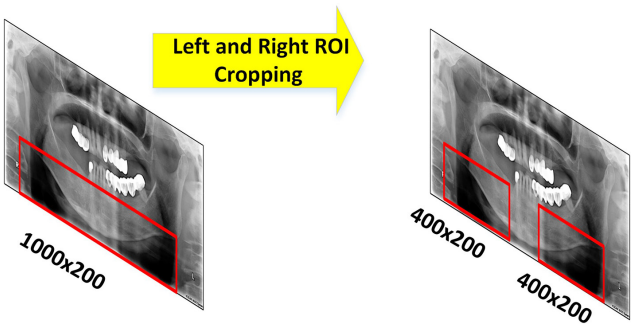

Figure 3 Data preparation for MC-DCNN. From the 1000 × 200-pixel ROI extracted in Figure 1, two ROIs, each 400 × 200 pixels in size, are extracted from the left and right jawline areas. MC-DCNN, multicolumn deep convolutional neural network; ROI, region of interest.

Training the SC-DCNN and MC-DCNN

Both the SC-DCNN and MC-DCNN were trained using Theano[38] on a single NVIDIA GTX980 GPU. For fair comparison between the two methods, similar training protocols were used as follows:

The parameter θ of the network was initialised using the Xavier[39] initialisation method. As the output of the network was interpreted as the model for the conditional distribution over the two classes, the training criteria were to maximise the probability of the true category in the training data D or the equivalent, and to minimize the negative log-likelihood loss $l(\theta, D)$, given as in equation (2).

$$l\left(\theta, D\right) = -\sum_{i=0}^{|D|} \log\left(P\left(Y = y^{(i)}|x^{(i)}, \theta\right)\right) \qquad (2)$$

where $P\left(Y = y^{(i)}|x^{(i)}, \theta\right)$ is the probability that the i*th* input data $x^{(i)}$ belong to the true class $y^{(i)}$. To optimise the loss function, the network was trained using Adams,[40] with a learning rate of 0.001 and a mini-batch size of 24. In the absence of a large training dataset, deep neural networks are susceptible to overfitting owing to their capacity. To reduce overfitting, we regularised the network by using the following methods:

(1) Dropout[41] ($p = 0.5$) was applied to the first two fully connected layers.
(2) L1 ($\lambda_1 = 0.0001$) and L2 ($\lambda_2 = 0.0001$) regularisation were applied to the kernels in all the convolutional layers.

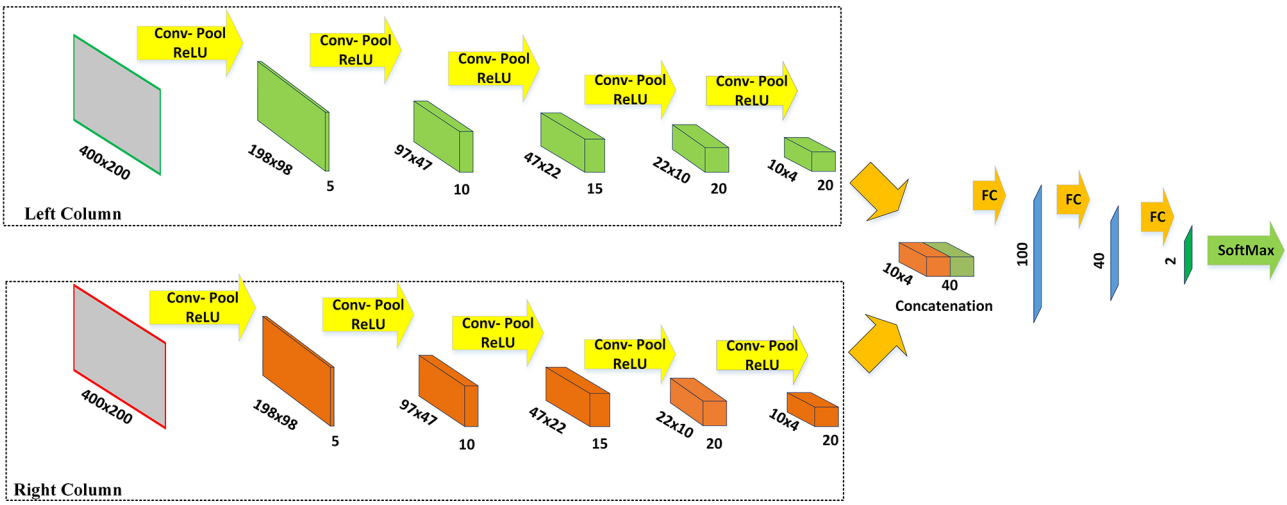

Figure 4 MC-DCNN for panoramic radiograph classification. MC-DCNN, multicolumn deep convolutional neural network.

Despite the relatively small training sample size, the applied regularisation methods prevented overfitting of the model. The test results showed that the models using both the SC-DCNN and MC-DCNN for training generalised well and thus did not overfit. We also augmented the training set of SC-DCNN by flipping the panoramic radiographs horizontally, which increased the amount of training data by a factor of two, by training another single-column network on this dataset. The data augmentation influenced the performance of this network, henceforth referred as SC-DCNN (Augment). The trained SC-DCNN (without Augment), SC-DCNN (Augment) and MC-DCNN were tested with 200 panoramic radiographs interpreted as either normal or osteoporosis from the test set, including 100 from the normal group and 100 from the osteoporosis group.

Results

The diagnostic performance of the trained models was evaluated on the test set consisting of 100 panoramic radiographs each from the normal and osteoporosis groups. The confusion matrix of the SC-DCNN classifier is presented in Table 1. Table 2 shows the confusion matrix of the MC-DCNN on the same test set. The confusion matrix of SC-DCNN (Augment) is presented in Table 3. The diagnostic performance of the SC-DCNN (without Augment), MC-DCNN and SC-DCNN (with Augment) are evaluated in terms of accuracy, precision, recall, F1 score and area under the curve (AUC). The results for diagnostic performance of the SC-DCNN and MC-DCNN are shown in Table 4.

The receiver operating curves of the three networks are shown in Figure 5, where the area under the curve of the SC-DCNN (without Augment) was 0.9763, that of the MC-DCNN was 0.9987 and that of SC-DCNN (Augment) was 0.9991 (Figure 5).

Discussion

The CAD system is an interdisciplinary technology that combines elements of AI and computer vision with radiological image processing.[42] It has been integrated as part of the PACS.[43] This increased the reader sensitivity with minimal reading time, thus improving the efficiency in daily clinical practice.[43]

Panoramic radiography is commonly performed by dentists. This radiographic examination allows for the evaluation of dentition and adjacent structures. A CAD system based on panoramic radiography has been developed for screening systemic diseases such as osteoporosis and carotid artery calcification.[18,26–29,44,45]

Osteoporosis has been characterised as a silent disease because patients cannot recognise weakening of their bones until a fracture occurs. According to the Korea National Health and Nutrition Examination Survey 2008–2011, 75.3% of responders aged ≥50 years were underdiagnosed and unconcerned about osteoporosis.[7]

Table 1 Confusion matrix of the SC-DCNN (without data augmentation) on the test

Actual (↓) / Predicted (→)	*Normal*	*Osteoporosis*	*AUC*
Normal	89	11	0.9763
Osteoporosis	4	96	

AUC, area under the curve; SC-DCNN, single-column deep convolutional neural network.

Table 2 Confusion matrix of the MC-DCNN (without data augmentation) on the test

Actual (↓) / Predicted (→)	*Normal*	*Osteoporosis*	*AUC*
Normal	97	3	0.9987
Osteoporosis	0	100	

AUC, area under the curve; MC-DCNN, multicolumn deep convolutional neural network.

Table 3 Confusion matrix of the SC-DCNN (with data augmentation) on the test

Actual (↓) / Predicted (→)	*Normal*	*Osteoporosis*	*AUC*
Normal	96	4	0.9991
Osteoporosis	0	100	

AUC, area under the curve; SC-DCNN, single-column deep convolutional neural network.

Therefore, development of an effective CAD system for detecting osteoporosis based on panoramic radiography could help general dentists readily inform patients of the possibility of osteoporosis and enable patients to begin early treatments.

Some researchers presented a fuzzy neural network-based diagnosis method for osteoporosis.[28] Fuzzy rules were built using various features of images. Combined with the generalisation property of neural networks, their system covers more area, including those missed by fuzzy rules. However, this approach is valid only when image features are extracted accurately using sophisticated pre-processing algorithms. If images are taken from unfamiliar environments or with unexpected noise added to the images, the system might easily create errors. To resolve this problem, many researchers have struggled to develop robust and automatic feature extraction algorithms by using various computer-aided approaches.[18,44,46] However, a satisfactory solution has not yet been reached.

A study was conducted on building optimal rules of a fuzzy algorithm by using a genetic algorithm.[29] A better set of rules was found via the crossover, mutation and selection procedures of the genetic algorithm. However, this approach still does not overcome a drawback; that is, finding the optimal rules with the best parameters is not guaranteed. Therefore, some other method that overcomes all the above-mentioned limitations is needed. The neural network satisfies these requirements, in which all the required knowledge for a diagnosis is built only with training data. Recently, a cutting-edge neural network technology called deep learning was developed and it has shown a performance level equal or even superior to that of human readers.

Table 4 Diagnostic performance of the SC-DCNN and MC-DCNN

Methods	*Accuracy*	*Precision*	*Recall*	*F1 score*	*AUC*
SC-DCNN (without Augment)	92.5%	0.957	0.89	0.922	0.9763
SC-DCNN (with Augment)	98%	1.0	0.96	0.979	0.9991
MC-DCNN	98.5%	1.0	0.97	0.985	0.9987

AUC, area under the curve; MC-DCNN, multicolumn deep convolutional neural network; SC-DCNN, single-column deep convolutional neural network.
Accuracy = TP+ TN/TP+FP+FN+TN; Precision = TP/TP+FP; Recall = TP/TP+FN; F1 score = 2*(recall * precision)/(recall + precision); TP (true positive); TN (true negative); FP (false positive); FN (false negative).

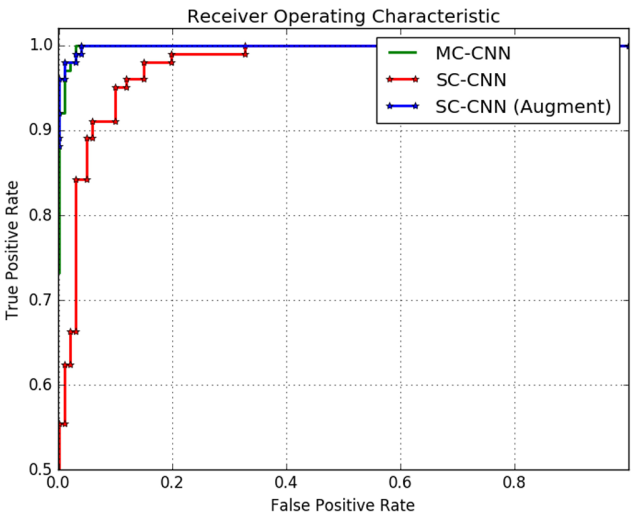

Figure 5 ROC curves of the single-column and multicolumn convolutional neural networks. ROC, receiver operating characteristic.

Previous CAD systems that used machine learning for the detection of osteoporosis based on panoramic radiography showed variable diagnostic performance in terms of sensitivity and specificity.[26–29] The sensitivity and specificity obtained in this study were much higher than those in previous studies.[26–29] Previous studies showed that once the CAD system diagnosed osteoporosis, it recorded sensitivity and specificity by comparing these with the BMD measurement from either the lumbar spine or femoral neck. In our study, the system recorded both sensitivity and specificity based on a comparison with the reports by oral and maxillofacial radiologists. Although the diagnosis of osteoporosis relied on the subjective interpretation of panoramic radiographs by observers, this DCNN-based CAD system showed excellent agreement with the oral and maxillofacial radiologists. MC-DCNN and SC-DCNN (Augment) were better than the SC-DCNN in terms of identifying more meaningful features for classifying panoramic radiographs.

This diagnostic performance of the DCNN-based CAD system may detect osteoporosis more efficiently based on different aspects of a patient's panoramic radiograph, which might be missed by a human observer. Therefore, further studies will be needed to compare the diagnostic performance between the DCNN-based CAD system and oral and maxillofacial radiologists.

The present study had several limitations. First, there was a lack of a gold standard for making a diagnosis of osteoporosis in each of the cases. Second, we did not have access to certain medical data from the subjects. For example, menstruation history and hormone replacement therapy, which affect bone metabolism, were not documented. However, a previous study revealed a high accuracy of clearly eroded inferior cortex of the mandible in detecting osteoporosis.[19,47]

Furthermore, following the study of Klemetti et al, several studies have also demonstrated a significant

association between mandibular cortical shape on panoramic radiographs and skeletal BMD on DXA in post-menopausal females.[13–19]

As the DCNN architecture generally involves many layers in its neural network, large quantities of sample image data are necessary when training convolutional neural networks.[48] Such a large data set is difficult to find in the medical field. Initial studies that involve the use of DCNNs are available in the medical field.[49] Generally, over 1000 images are used for training of deep learning systems for medical radiological images. However, with data augmentation and reuse of the pre-trained network, about 100 cases per class could provide an acceptable outcome.[50]

In conclusion, our DCNN-based CAD system (connectionist AI) is useful for detecting osteoporosis, and even with a smaller number of radiological images designed for learning, it can achieve excellent precision. The MC-DCNN outperformed the SC-DCNN (without Augment) in terms of accuracy, as determined by their respective ROC. In addition, the performance of the SC-DCNN (Augment) improved due to training data augmentation, and was comparable to that of the MC-DCNN. A DCNN-based CAD system could provide information to dentists for the early detection of osteoporosis, and asymptomatic patients with osteoporosis can then be referred to the appropriate medical professionals.

Funding

This study was supported in part by a grant (CRI 18028–1) Chonnam National University Hospital Biomedical Research Institute, the Korea Research Fellowship Program funded by the Ministry of Science and ICT through the National Research Foundation of Korea (NRF-2015H1D3A1062316), and Basic Science Research Program through the National Research Foundation of Korea (NRF) funded by the Ministry of Education (NRF-2016R1A2B4015514).

References

1. Consensus development conference: prophylaxis and treatment of osteoporosis. *Am J Med* 1991; **90**: 107–10.
2. Cauley JA. Public health impact of osteoporosis. *J Gerontol A Biol Sci Med Sci* 2013; **68**: 1243–51. doi: https://doi.org/10.1093/gerona/glt093
3. Hernlund E, Svedbom A, Ivergård M, Compston J, Cooper C, Stenmark J, et al. Osteoporosis in the European Union: medical management, epidemiology and economic burden. A report prepared in collaboration with the International Osteoporosis Foundation (IOF) and the European Federation of Pharmaceutical Industry Associations (EFPIA). *Arch Osteoporos* 2013; **8**: 136. doi: https://doi.org/10.1007/s11657-013-0136-1
4. Lee YK, Yoon BH, Koo KH. Epidemiology of osteoporosis and osteoporotic fractures in South Korea. *Endocrinol Metab* 2013; **28**: 90–3. doi: https://doi.org/10.3803/EnM.2013.28.2.90
5. Bliuc D, Nguyen ND, Nguyen TV, Eisman JA, Center JR. Compound risk of high mortality following osteoporotic fracture and refracture in elderly women and men. *J Bone Miner Res* 2013; **28**: 2317–24. doi: https://doi.org/10.1002/jbmr.1968
6. Looker AC, Melton LJ. 3rd, Harris TB, Borrud LG, Shepherd JA. Prevalence and trends in low femur bone density among older US adults: NHANES 2005-2006 compared with NHANES III. *J Bone Miner Res* 2010; **25**: 64–71.
7. Kim Y. Osteoporosis or Low Bone Mass in Adults Aged 50 years old and above in Republic of Korea, 2008-2011. 2017. Available from: http://cdc.go.kr/CDC/info/CdcKrInfo0301.jsp?menuIds=HOME001-MNU1154-MNU0005- MNU0037&cid=21375 [cited 2017 June 16].
8. U.S. Preventive Services Task Force. Screening for osteoporosis: U.S. preventive services task force recommendation statement. *Ann Intern Med* 2011; **154**: 356–64. doi: https://doi.org/10.7326/0003-4819-154-5-201103010-00307
9. Lim LS, Hoeksema LJ, Sherin K, ACPM Prevention Practice Committee. Screening for osteoporosis in the adult U.S. population: ACPM position statement on preventive practice. *Am J Prev Med* 2009; **36**: 366–75. doi: https://doi.org/10.1016/j.amepre.2009.01.013
10. Riggs BL, Melton LJ. Involutional osteoporosis. *N Engl J Med* 1986; **314**: 1676–86. doi: https://doi.org/10.1056/NEJM198606263142605
11. Mithal ADV, Lau E. *The Asian Audit. Epidemiology, costs and burden of osteoporosis in Asia*. International Osteoporosis Foundation; 2009.
12. Gomes CC, de Rezende Barbosa GL, Bello RP, Bóscolo FN, de Almeida SM. A comparison of the mandibular index on panoramic and cross-sectional images from CBCT exams from osteoporosis risk group. *Osteoporos Int* 2014; **25**: 1885–90. doi: https://doi.org/10.1007/s00198-014-2696-3
13. White SC, Taguchi A, Kao D, Wu S, Service SK, Yoon D, et al. Clinical and panoramic predictors of femur bone mineral density. *Osteoporos Int* 2005; **16**: 339–46. doi: https://doi.org/10.1007/s00198-004-1692-4
14. Yaşar F, Akgünlü F. The differences in panoramic mandibular indices and fractal dimension between patients with and without spinal osteoporosis. *Dentomaxillofac Radiol* 2006; **35**: 1–9. doi: https://doi.org/10.1259/dmfr/97652136
15. Taguchi A, Ohtsuka M, Tsuda M, Nakamoto T, Kodama I, Inagaki K, et al. Risk of vertebral osteoporosis in post-menopausal women with alterations of the mandible. *Dentomaxillofac Radiol* 2007; **36**: 143–8. doi: https://doi.org/10.1259/dmfr/50171930
16. Taguchi A, Ohtsuka M, Nakamoto T, Naito K, Tsuda M, Kudo Y, et al. Identification of post-menopausal women at risk of osteoporosis by trained general dental practitioners using panoramic radiographs. *Dentomaxillofac Radiol* 2007; **36**: 149–54. doi: https://doi.org/10.1259/dmfr/31116116
17. Okabe S, Morimoto Y, Ansai T, Yoshioka I, Tanaka T, Taguchi A, et al. Assessment of the relationship between the mandibular cortex on panoramic radiographs and the risk of bone fracture and vascular disease in 80-year-olds. *Oral Surg Oral Med Oral Pathol Oral Radiol Endod* 2008; **106**: 433–42. doi: https://doi.org/10.1016/j.tripleo.2007.09.013
18. Devlin H, Karayianni K, Mitsea A, Jacobs R, Lindh C, van der Stelt P, et al. Diagnosing osteoporosis by using dental panoramic radiographs: the OSTEODENT project. *Oral Surg Oral Med Oral Pathol Oral Radiol Endod* 2007; **104**: 821–8. doi: https://doi.org/10.1016/j.tripleo.2006.12.027
19. Klemetti E, Kolmakov S, Kröger H. Pantomography in assessment of the osteoporosis risk group. *Scand J Dent Res* 1994; **102**: 68–72. doi: https://doi.org/10.1111/j.1600-0722.1994.tb01156.x

20. Ledgerton D, Horner K, Devlin H, Worthington H. Radiomorphometric indices of the mandible in a British female population. *Dentomaxillofac Radiol* 1999; **28**: 173–81. doi: https://doi.org/10.1038/sj.dmfr.4600435
21. Taguchi A, Suei Y, Ohtsuka M, Otani K, Tanimoto K, Ohtaki M. Usefulness of panoramic radiography in the diagnosis of postmenopausal osteoporosis in women. Width and morphology of inferior cortex of the mandible. *Dentomaxillofac Radiol* 1996; **25**: 263–7. doi: https://doi.org/10.1259/dmfr.25.5.9161180
22. Miliuniene E, Alekna V, Peciuliene V, Tamulaitiene M, Maneliene R. Relationship between mandibular cortical bone height and bone mineral density of lumbar spine. *Stomatologija* 2008; **10**: 72–5.
23. Al-Dam A, Blake F, Atac A, Amling M, Blessmann M, Assaf A, et al. Mandibular cortical shape index in non-standardised panoramic radiographs for identifying patients with osteoporosis as defined by the German Osteology Organization. *J Craniomaxillofac Surg* 2013; **41**: e165–e169. doi: https://doi.org/10.1016/j.jcms.2012.11.044
24. Taguchi A, Tsuda M, Ohtsuka M, Kodama I, Sanada M, Nakamoto T, et al. Use of dental panoramic radiographs in identifying younger postmenopausal women with osteoporosis. *Osteoporos Int* 2006; **17**: 387–94. doi: https://doi.org/10.1007/s00198-005-2029-7
25. Taguchi A. Triage screening for osteoporosis in dental clinics using panoramic radiographs. *Oral Dis* 2010; **16**: 316–27. doi: https://doi.org/10.1111/j.1601-0825.2009.01615.x
26. Roberts MG, Graham J, Devlin H. Image texture in dental panoramic radiographs as a potential biomarker of osteoporosis. *IEEE Trans Biomed Eng* 2013; **60**: 2384–92. doi: https://doi.org/10.1109/TBME.2013.2256908
27. Kavitha MS, Asano A, Taguchi A, Kurita T, Sanada M. Diagnosis of osteoporosis from dental panoramic radiographs using the support vector machine method in a computer-aided system. *BMC Med Imaging* 2012; **12**: 1. doi: https://doi.org/10.1186/1471-2342-12-1
28. Arifin AZ, Asano A, Taguchi A, Nakamoto T, Ohtsuka M, Tsuda M, et al. Use of Fuzzy Neural Network in Diagnosing Postmenopausal Women with Osteoporosis Based on Dental Panoramic Radiographs. *JACIII* 2007; **11**: 1049–58. doi: https://doi.org/10.20965/jaciii.2007.p1049
29. Kavitha MS, Ganesh Kumar P, Park SY, Huh KH, Heo MS, Kurita T, et al. Automatic detection of osteoporosis based on hybrid genetic swarm fuzzy classifier approaches. *Dentomaxillofac Radiol* 2016; **45**: 20160076. doi: https://doi.org/10.1259/dmfr.20160076
30. Boden MA. *AI: Its nature and future*. Oxford University Press; 2016.
31. Russakovsky O, Deng J, Su H, Krause J, Satheesh S, Ma S, et al. ImageNet large scale visual recognition challenge. *Int J Comput Vis* 2015; **115**: 211–52. doi: https://doi.org/10.1007/s11263-015-0816-y
32. He K, Zhang X, Ren S, Sun J. *Deep residual learning for image recognition. Proceedings of the IEEE conference on computer vision and pattern recognition; 2016*; 2016. pp. 770–8.
33. Cheng JZ, Ni D, Chou YH, Qin J, Tiu CM, Chang YC, et al. Computer-aided diagnosis with deep learning architecture: applications to breast lesions in US images and pulmonary nodules in CT scans. *Sci Rep* 2016; **6**: 24454. doi: https://doi.org/10.1038/srep24454
34. Hua KL, Hsu CH, Hidayati SC, Cheng WH, Chen YJ. Computer-aided classification of lung nodules on computed tomography images via deep learning technique. *Onco Targets Ther* 20152015; **8**: 22; **8**: 22. doi: https://doi.org/10.2147/OTT.S80733
35. Liu S, Liu S, Cai W, Pujol S, Kikinis R, Feng D. Early diagnosis of Alzheimer's disease with deep learning. Biomedical Imaging (ISBI), 2014 IEEE 11th International Symposium on; 2014. *IEEE* 2014; 1015–8.
36. Krizhevsky A, Sutskever I, Hinton GE. Imagenet classification with deep convolutional neural networks. *Adv Neural Inf Process Syst* 2012; **2012**: 1097–105.
37. Glorot X, Bordes A, Bengio Y. Deep sparse rectifier neural networks. Proceedings of the Fourteenth International Conference on Artificial Intelligence and Statistics; 2011. 2011; 315–23.
38. Bergstra J, Breuleux O, Bastien F, Lamblin P, Pascanu R, Desjardins G. Theano: A CPU and GPU math compiler in Python. Proc 9th Python in Science Conf; 2010. 2010; 1–7.
39. Glorot X, Bengio Y. Understanding the difficulty of training deep feedforward neural networks. Proceedings of the Thirteenth International Conference on Artificial Intelligence and Statistics; 2010. 2010; 249–56.
40. Kingma D, Ba J. Adam: a method for stochastic optimization. *arXiv preprint arXiv* 2014;: 14126980.
41. Srivastava N, Hinton GE, Krizhevsky A, Sutskever I, Salakhutdinov R. Dropout: a simple way to prevent neural networks from overfitting. *J Mach Learn Res* 2014; **15**: 1929–58.
42. Wikipedia. Computer-aided diagnosis. 2017. Available from: https://en.wikipedia.org/wiki/Computer-aided_diagnosis [cited 2017 July 21].
43. Bogoni L, Ko JP, Alpert J, Anand V, Fantauzzi J, Florin CH, et al. Impact of a computer-aided detection (CAD) system integrated into a picture archiving and communication system (PACS) on reader sensitivity and efficiency for the detection of lung nodules in thoracic CT exams. *J Digit Imaging* 2012; **25**: 771–81. doi: https://doi.org/10.1007/s10278-012-9496-0
44. Kavitha MS, Asano A, Taguchi A, Heo MS. The combination of a histogram-based clustering algorithm and support vector machine for the diagnosis of osteoporosis. *Imaging Sci Dent* 2013; **43**: 153–61. doi: https://doi.org/10.5624/isd.2013.43.3.153
45. Sawagashira T, Hayashi T, Hara T, Katsumata A, Muramatsu C, Zhou X, et al. An automatic detection method for carotid artery calcifications using top-hat filter on dental panoramic radiographs. *Conf Proc IEEE Eng Med Biol Soc* 2011; **2011**: 6208–11. doi: https://doi.org/10.1109/IEMBS.2011.6091533
46. Arifin AZ, Asano A, Taguchi A, Nakamoto T, Ohtsuka M, Tsuda M, et al. Computer-aided system for measuring the mandibular cortical width on dental panoramic radiographs in identifying postmenopausal women with low bone mineral density. *Osteoporos Int* 2006; **17**: 753–9. doi: https://doi.org/10.1007/s00198-005-0045-2
47. Gaur B, Chaudhary A, Wanjari PV, Sunil M, Basavaraj P. Evaluation of panoramic radiographs as a screening tool of osteoporosis in post menopausal women: a cross sectional study. *J Clin Diagn Res* 2013; **7**: 2051–5. doi: https://doi.org/10.7860/JCDR/2013/5853.3403
48. Oquab M, Bottou L, Laptev I, Sivic J. Learning and transferring mid-level image representations using convolutional neural networks. *Proceedings of the IEEE conference on computer vision and pattern recognition* 2014; **2014**: 1717–24.
49. Cireşan DC, Giusti A, Gambardella LM, Schmidhuber J. *Mitosis detection in breast cancer histology images with deep neural networks. International Conference on Medical Image Computing and Computer-assisted Intervention; 2013*: Springer; 2013. pp. 411–8.
50. Lee JG, Jun S, Cho YW, Lee H, Kim GB, Seo JB, et al. Deep learning in medical imaging: general overview. *Korean J Radiol* 2017; **18**: 570–84. doi: https://doi.org/10.3348/kjr.2017.18.4.570